03.2

Numerical and experimental study of the effect of gas blowing/suction through a perforated surface on the boundary layer at a supersonic Mach number

© P.A. Polivanov

Khristianovich Institute of Theoretical and Applied Mechanics, Siberian Branch, Russian Academy of Sciences, Novosibirsk, Russia
E-mail: polivanov@itam.nsc.ru

Received May 11, 2021
Revised July 12, 2021
Accepted July 16, 2021

In this paper a numerical and experimental study of the effect of blowing/suction through a perforated surface on a turbulent boundary layer at a Mach number M = 1.4 was carried out. Most of the calculations were performed by Reynolds-averaged Navier–Stokes equations with the $\kappa-\omega$ SST turbulence model. The calculated geometry completely repeated the experimental one including the perforated surface. The numerical data were compared with experimental measurements obtained by the PIV method. Analysis of the data made it possible to find the limits of applicability of the numerical method for the flow under study.

Keywords: supersonic flow, gas blowing/suction through a perforated surface, boundary layer, turbulence model $\kappa-\omega$ SST, PIV method.

DOI: 10.21883/TPL.2022.14.52056.18862

The gas blowing/suction through a perforated (porous) surface is widely used in various tasks of aeronautical engineering (e.g., walls cooling, boundary layer control, separated flows, etc.). The major theoretical and experimental investigations of using blowing/suction through the perforated surfaces in the gas dynamic problems were performed for subsonic speeds [1,2]. The number of experimental studies in the field of using blowing/suction through the perforated surfaces for supersonic flows is essentially lower. In these tasks, a change of the flow pattern due to blowing/suction through pores is typically investigated, and variations in different characteristics of the boundary layer near the perforated surface (e.g., displacement thickness, shape factor, etc.) are usually ignored. For instance, authors of [3] used porous surfaces to control separated flows, however, detailed analysis of the flow near porous inserts and porosity geometry effect was not performed. In [4], dimensionless dependences of the mass flowrate through the porous surface for the boundary layer suction devices versus the perforated surface geometry were found out, but no detailed data on changes in the boundary layer condition were presented. At present, the flow structure in interaction between a single jet and supersonic flow is well studied. For instance, paper [5] presents data obtained for the case of a highly underexpanded jet. However, the flow structure was not thoroughly studied for perforated surfaces in the boundary layer zone in the process of blowing/suction.

The task of active control of trans- and supersonic flows is critically important for ensuring further progress in the aviation industry. Most of control methods are based on modifying the boundary layer. For instance, in studies [6,7] plasma actuators were used to suppress the separation zones by intensifying the mass exchange between the external flow and boundary layer [6] or by turbulizing the flow [7]. In solving these tasks, the interest in using blowing/suction through the perforated surface is reduced to more detailed consideration of the technological aspects of the issue. This enables fast implementation of this technique into real applications. The more active utilization of this technique needs proper understanding of the physics of the blowing/suction effect on the boundary layer depending on the perforated layer geometry and flow parameters.

Since experimental investigation needs essential resources, numerical methods are preferable. The eddy-resolving numerical methods (LES/DNS) allow calculation of these flows [8] but need much computational time. Methods based on the Reynolds equation (RANS) need considerably lower computational resources, which makes them quite attractive for solving this task, however, the used hypotheses and empirical nature of coefficients involved in the RANS turbulence model make it necessary to verify the calculations. Hence, it was decided to perform a combined calculation-experimental study aimed at verifying the RANS methods used in solving problems of the effect of blowing/suction through the perforated surface on the supersonic boundary layer.

The experiments were conducted in aerodynamic tube T-327b modified for low supersonic numbers. As an experimental setup, an expanding test section 370 mm long with a rectangular cross-section (57 mm wide, 19 to 23 mm high) was used. In front of the duct, a flat Laval nozzle designed for Mach number M = 1.4 was installed. The test section was expanded in order to compensate the effect of the increase in the boundary layer thickness

along the duct. Fig. 1 presents the setup drawing. The experiments were carried out at the stagnation temperature $T_0 = 298$ K and stagnation pressure $P_0 = 1.01 \cdot 10^5$ Pa ($\mathrm{Re}_1 \approx 15 \cdot 10^6\,\mathrm{m}^{-1}$). To ensure optical access to the measurement zone, two windows were made in the duct side walls. On the upper wall there were two grooves for mounting the perforated inserts. The first was made near the nozzle edge, the other was in the center of the duct in the zone of the developed turbulent boundary layer. To make the boundary layer turbulent, a turbulizer was mounted along the entire duct at the nozzle outlet. As the turbulizer, a sandpaper strip 0.2 mm high and 1.5 mm long was used, which occupied the entire width of the operating section. The bottom wall was made from Plexiglas allowing delivering laser radiation to the area under study. The main measurement technique was the PIV (particle image velocimetry) method. The flow was impregnated with microparticles with the average size of 1 μm. Random error of instantaneous speed vector measurements did not exceed 2% in these experiments. The startup time was ~ 50 s. The statistics was estimated based on 700 instantaneous speed fields.

The blowing and suction were organized by connecting the insert with perforated surface to either a high-pressure chamber or a vacuum one by using a corrugated hose. The gas flowrate was controlled with different ball valves. The open cross-section area of the valves used did not exceed the total area of holes on the porous insert surface. This fact, as well as ensuring the required pressure difference, resulted in formation in the section of the ball valve Mach number $\mathrm{M} = 1$. Taking into account the data on the stagnation temperature and pressure before this section, the gas flowrate $R = S_{cr} a_{cr} \rho_{cr}$ was calculated (here a_{cr}, ρ_{cr}, S_{cr} are the sound speed, density, and area of the aperture at the Mach number $\mathrm{M} = 1$, respectively). In addition, the air mass-flow rate through the corrugated hose was measured with flow meter Honeywell AWM720P1. The difference in the results of two air flowrate measurement methods did not exceed 10%.

The numerical simulation was performed in the 3D RANS version using the ANSYS Fluent code. The computational domain fully coincided with the duct geometry under study, including the perforated insert (all the insert holes were modeled). A structured blocked grid was used. Based on the results of the grid convergence analysis, the following grid parameters were selected: $y^+ \approx 1$, $x^+ \approx 10$, $z^+ \approx 10$, total number of the grid nodes of ~ 8 mln, number of meshes in the vicinity of one hole of ~ 200 (in the plane perpendicular to the cylindrical hole symmetry axis). To accelerate the computation, only a duct section 100 mm long was modeled (Fig. 1). The inflow boundary conditions were set to values obtained based on preliminary calculations for the entire duct up to the perforated zone, including a part of the prechamber and Laval nozzles. In modeling blowing/suction, the boundary condition of the constant mass flow rate was established in the lower part of the porous insert. In the ANSYS Fluent code, this

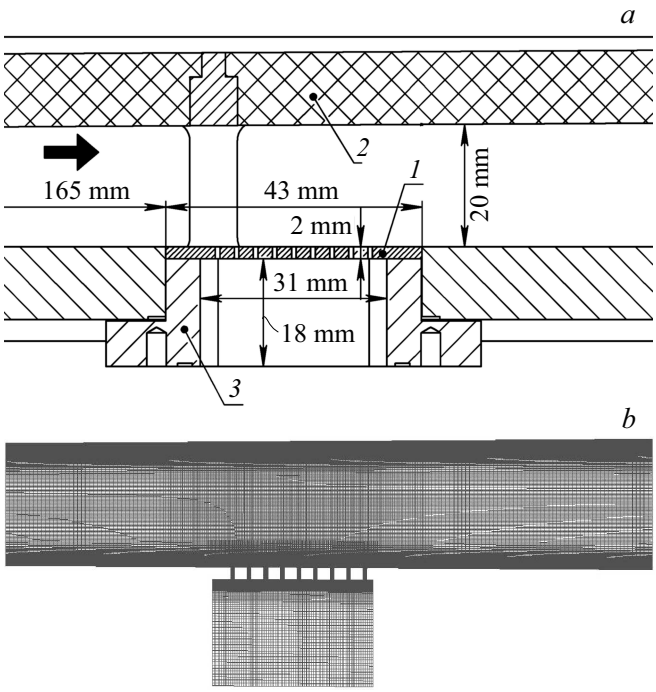

Figure 1. *a* — A sketch of the experimental setup in the zone of the perforated insert. *1* — perforated wall, *2* — optical window, *3* — insert. *b* — computational space.

boundary condition is realized by automatically fitting the static pressure ensuring the preset gas flowrate. Preliminary calculations showed that the best agreement between the experimental and numerical results is observed in using the κ–ω SST turbulence model just that was further used in numerical simulation. To determine the possible contribution to the main flow from nonstationary large-scale structures formed in the blowing/suction zone, it was decided to perform a part of calculations with the IDDES (improved delayed detached eddy simulation) approach using the subgrid turbulence model κ–ω SST. In the IDDES approach, the same stationary conditions as in the RANS calculations were established. In the IDDES model, nonstationary processes emerged only in the blowing zone.

In the experimental and numerical studies, various perforated inserts with different hole diameters and interhole intervals were considered. Detailed description of the perforated inserts is given in [9]. In this work, the order of numbering of the perforated inserts is the same as in [9]. This paper presents the results obtained for inserts with #4 ($d = 0.8$ mm, $h = 1.6$ mm) and #7 ($d = 2$ mm, $h = 4$ mm), where d is the hole diameter, h is the interhole distance. Fig. 2 demonstrates the example of data obtained for gas blowing. The end of the porous insert was assumed to be the zero longitudinal coordinate. Coordinates X^* and Y^* were made dimensionless by normalizing them by the boundary layer displacement thickness at the end of the porous insert obtained without blowing/suction. The perforated zone ends near $X^* = -10$.

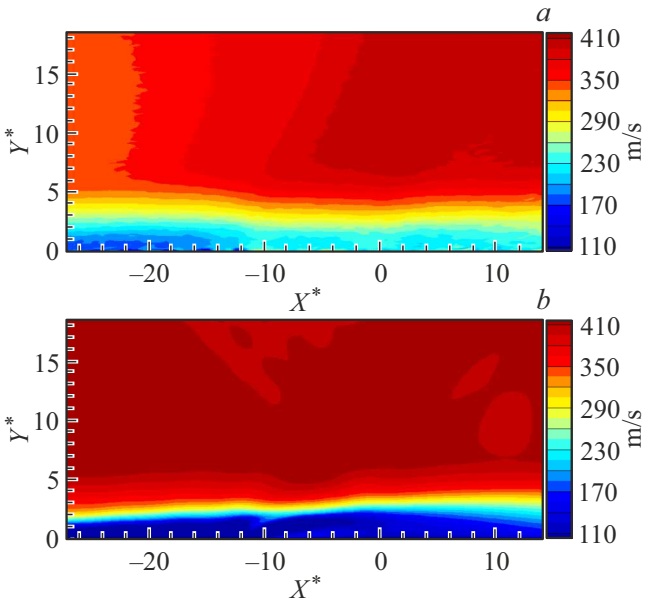

Figure 2. Comparison of the experimental and theoretical streamwise speed fields obtained for the porous insert #7 at the gas flowrate $R/R_d = 0.22$. *a* — experiment, *b* — κ–ω SST.

Fig. 2 clearly demonstrates that a region with a lower flow speed is formed in the boundary layer near the wall in the zone of flow blowing. The experimental data exhibits a greater fullness of the velocity profile in this region as compared with the numerical data. In the outer part of the flow, the experimentally obtained flow speed is lower than the calculated one. The reason for the flow speed decrease out of the boundary layer is a shock wave generated at the beginning of the blowing zone. At the end of the blowing region, the displacement thickness decreases sharply, which results in formation of an expansion fan. As a result, the flow speed in the duct increases again. The calculation also exhibited the emergence of the shock wave and expansion wave, however, their intensity was much less than in the experiment. As a result, the flow patterns in the duct are qualitatively different. It may be assumed that one of the reasons for that difference is the problem of modeling the interaction between the arising shock wave and boundary layer. According to the RANS calculation, a slow increase in the fullness of the velocity profile is observed in the zone of wake (behind the porous insert). In the experimental data, the turbulent boundary layer at the end of the measurement region is closer to the equilibrium state than in the calculations. Notice that in the blowing zone the IDDES calculations give average flow fields similar to the RANS calculations, but in the zone of wake (behind the porous insert) IDDES data are closer to the experimental results. Assumably, this is because of large eddies arising in the blowing zone in the IDDES calculation. The large-scale eddy structures enhanced the convective processes in the boundary layer, which made faster the increase in the wake fullness of the velocity profiles. The decrease in the mass

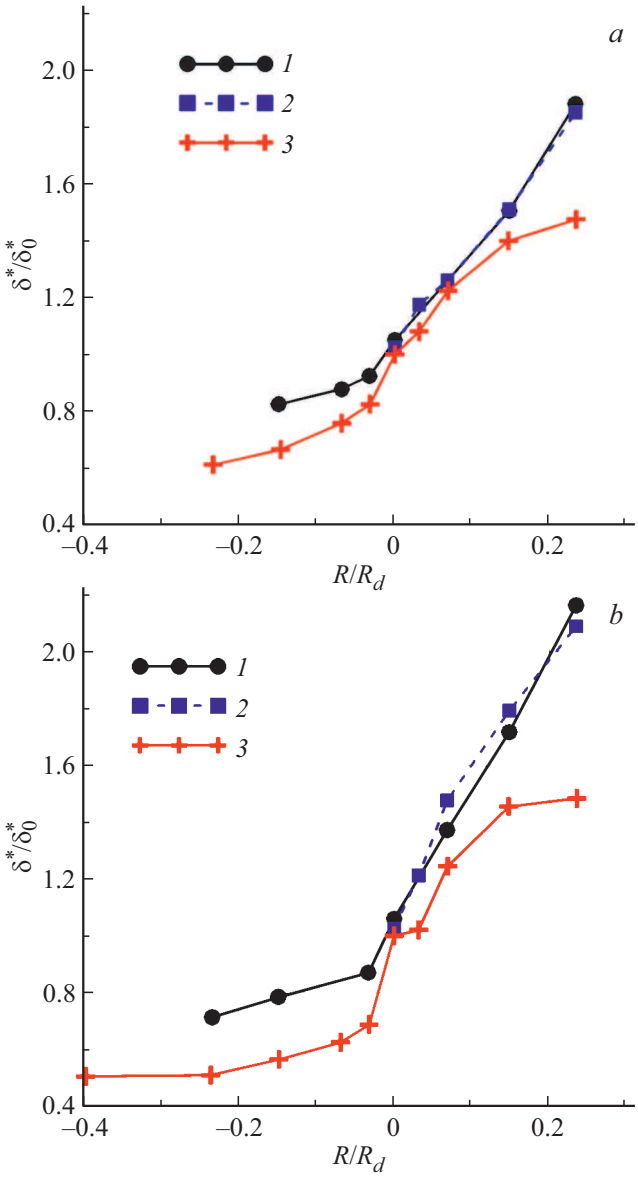

Figure 3. Comparison of the experimental and theoretical data in the cross-section $X/\delta_0^* = -21$ for the porous insert #4 (*a*) and #7 (*b*). *1* — κ–ω SST, *2* — IDDES, *3* — experiment.

flowrate through the porous insert led to a decrease in the difference between the calculations and measurements. The flow patterns obtained at other porous insert parameters are qualitatively consistent with Fig. 2.

Fig. 3 presents an example of comparison of integral data obtained from the perforated insert zone. Here, to make the data dimensionless, the displacement thickness obtained experimentally in the absence of blowing/suction (δ_0^*) and flowrate defined as $R_d = l\rho U\delta_0^*$ were used, where l is the porous insert width, U is the flow speed at the boundary layer edge, and ρ is the oncoming flow density. Both numerical methods exhibit a good data agreement within the entire flowrate range. In the downstream direction, gradual increase in difference between the IDDES

and RANS data is observed. The displacement thickness obtained in IDDES calculation is lower than that calculated by RANS and closer to the measurements. As mentioned above, the growth of the wake fullness of the velocity profile is, most probably, related with intense convective mass transfer processes in the IDDES calculation model, which are caused by nonstationary vortex structures arising in the blowing zone. In the zone of the perforated insert, the eddy effect is not insignificant yet, which makes the RANS and IDDES results similar to each other. Comparison of the calculations and experimental data shows good agreement at low mass flowrates through the perforated surface ($-0.05 < R/R_d \leqslant 0.1$). With increasing mass flowrate modulus, the difference between the theoretical and experimental data increases. At $|R/R_d| > 0.2$, the difference amounts up to 30% and more.

The flow suction is accompanied by formation of an expansion wave fan near the front edge of the porous insert. As a result, the boundary layer thickness decreases not only directly due to the gas suction but also due to the favorable pressure gradient. In the flow suction experiment, the displacement thickness variation decreases with increasing intensity of the mass-flow exchange through the perforated surface, which is most probably caused by the reduction of the favorable pressure gradient effect at high values of R. Notice that, in the case of flow suction, the difference between the calculations and measurements occurs at lower relative mass flowrates than in the case of blowing.

The boundary layer integral characteristics obtained for different geometries of the perforated insert are qualitatively similar. For instance, all the studied configurations demonstrated at high mass flowrates through the perforated surface an essential difference between the theoretical and experimental results. Since IDDES provides a better agreement between the calculated and experimental data, it is possible to assume that the data disagreement is caused by the problems in modeling large eddies in the boundary layer. The „engineering“ two-parameter RANS models employ the isotropic turbulence approach that, most likely, fails to take into account all the phenomena occurring in the zones of blowing/suction area. The nonstationary IDDES solver models the eddies directly, which allows taking into account anisotrpopy of the large-scale turbulence. This improves the data agreement in the wake but needs more computation time than the stationary method RANS. Since such an essential difference was not revealed in subsonic studies, assume that the non-equilibrium state of the turbulent boundary layer is caused by the shear flow interaction with local shock waves/expansion waves generated by local jets arising near the perforated insert holes. The cycle of works [10,11] devoted to studying the shock wave boundary — layer interaction has shown that the agreement between the experimental data and RANS calculations is observed mainly in simple 2D cases. Attempts to regard 3D effects result in the growth of difference between the calculations and measurements. These results indirectly evidence the existence of problems in RANS modeling of compressible flows with complex three-dimensional configurations. As an example, the task of blowing/suction through the perforated surface at the supersonic Mach number may be considered.

Comparison of the calculations and experimental data showed that the „engineering“ RANS approaches ensure good accuracy of modeling the effect of blowing/suction through perforated surfaces only at low relative mass flowrates ($-0.05 < R/R_d \leqslant 0.1$). At high mass flowrates, considerable differences between the experimental and theoretical data are observed. The obtained data show that the available one- and two-equation turbulence RANS models are essentially restricted in the case of simulating the blowing/suction through perforated surfaces at the supersonic Mach number.

Acknowledgements

The author is grateful to the Common Use Center „Mechanics“ for providing the necessary equipment.

Financial support

The study was financially supported by RSF (project 18-19-00547).

Conflict of interests

The author declares that he has no conflict of interests.

References

[1] V.I. Kornilov, Prog. Aerospace Sci., **76**, 1 (2015).
[2] A.V. Voevodin, A.A. Kornyakov, D.A. Petrov, A.S. Petrov, G.G. Sudakov, Tech. Phys. Lett., **44** (8), 687 (2018). DOI: 10.1134/S106378501808014X.
[3] *Drag reduction by shock and boundary layer control: results of the project EUROSHOCK II*, ed. by E. Stanewsky, J. Delery, J. Fulker, P. Matteis (Springer-Verlag, Berlin−Heidelberg, 2002), p. 452. DOI: 10.1007/978-3-540-45856-2
[4] R.A. Baurle, A.T. Norris, in *58th JANNAF Propulsion Meeting* (Arlington, VA, USA, 2011). https://ntrs.nasa.gov/search.jsp?R=20110011133
[5] A.O. Beketaeva, P. Bruel, A.Zh. Naimanova, Tech. Phys., **64** (10), 1430 (2019). DOI: 10.1134/S1063784219100049.
[6] A.A. Sidorenko, A.D. Budovsky, P.A. Polivanov, O.I. Vishnyakov, V.G. Sudakov, V.N. Ishchenko, Thermophys. Aeromech., **26** (4), 465 (2019). DOI: 10.1134/S0869864319040012.
[7] P.A. Polivanov, A.A. Sidorenko, Tech. Phys. Lett., **44** (9), 833 (2018). DOI: 10.1134/S1063785018090262.
[8] S. Ghosh, J.-I. Choi, J.R. Edwards, in *47th AIAA Aerospace Sciences Meeting including The New Horizons Forum and Aerospace Exposition* (Orlando, Florida, USA, 2009), AIAA Paper 2009-1330. DOI: 10.2514/6.2009-1330
[9] P.A. Polivanov, in *7th Eur. Conf. Aeronautics and Space Sciences (EUCASS 2017)* (Milano, Italy, 2017). DOI: 10.13009/EUCASS2017-351

[10] J.-P. Dussauge, R. Bur, T. Davidson, H. Babinsky, M. Bernardini, R. Giepman, F. Schrijer, B.V. Oudheusden, A. Sidorenko, & More Authors, in *Transition location effect on shock wave boundary layer interaction*, ed. by P. Doerffer, Ser. Notes on Numerical Fluid Mechanics and Multidisciplinary Design (Springer Open, 2021), vol. 144, p. 25. DOI: 10.1007/978-3-030-47461-4_2

[11] H. Babinsky, P. Dupont, P. Polivanov, A. Sidorenko, R. Bur, R. Giepman, F. Schrijer, B. van Oudheusden, A. Sansica, & More Authors, in Transition location effect on shock wave boundary layer interaction, ed. by P. Doerffer, Ser. Notes on Numerical Fluid Mechanics and Multidisciplinary Design (Springer Open, 2021), vol. 144, p. 129. DOI: 10.1007/978-3-030-47461-4_3